



REGULAR ARTICLE

# The effects of aluminum and silicon phosphates on thermal stability and flammability of polystyrene

ALLEN CHAPARADZA<sup>a</sup> and STEPHEN MAJONI<sup>b,\*</sup> 

<sup>a</sup>Department of Chemistry, Austin Peay State University, 601 College St, Clarksville, TN 37044, USA

<sup>b</sup>Department of Chemical and Forensic Sciences, Botswana International University of Science and Technology, P. Bag 16, Palapye, Botswana

E-mail: majonis@biust.ac.bw

MS received 21 April 2021; revised 8 September 2021; accepted 29 September 2021

**Abstract.** Polystyrene composites containing silicon orthophosphate, taranakite, and aluminum phosphate, were prepared *via* melt blending and characterized by powder X-ray diffraction, Fourier transform infrared spectroscopy, thermogravimetric analysis and cone calorimetry. The systematic investigations of the effects of the additives on flame retardancy, thermal decomposition, and pyrolysis behavior of polystyrene were conducted using cone calorimetry and thermogravimetric analysis. Thermogravimetric analysis indicated that the addition of aluminum phosphates caused small increases in thermal stability as evidenced by as low as 4 °C increase in onset degradation temperature and up to 13 °C increase in midpoint degradation temperature. The addition of silicon orthophosphate resulted in increases of between 9 and 27 °C in onset degradation temperature and between 13 and 31 °C in midpoint degradation temperature. Thermal stability increased with loading percentages, with 10 mass% giving the most stability. The addition of the additives at less than 10 weight percent resulted in a 22 to 52% reduction in the peak heat release rate. Whereas there is a significant reduction in the time-to-ignition for the phosphate composites compared to the virgin polymer, there are remarkable reductions in the peak heat release rate, average mass loss rate and smoke production.

**Keywords.** Silicon orthophosphate; Taranakite; Cone calorimetry; Flammability; Thermal stability.

## 1. Introduction

The demand for synthetic polymers has continued to grow and this has led to continuous research into polymer matrix composites (PMCs) that have improved mechanical, thermal, and electrical properties.<sup>1</sup> Modern technology has allowed optimization of PMCs to achieve a balance of properties for a given range of applications. Due to the lightweight, low cost and ease of processing of synthetic plastics, there has been an increase in the applications of plastics in a broad range of components in both domestic and industrial sectors. The resultant increase in the fire load fraction of plastics in the various sectors has led to enhanced research in the production of PMCs with a significantly lower tendency to ignite and burn easily compared to virgin polymers<sup>2,3</sup> as well as the development of flame retardant coatings.<sup>4,5</sup> Over the past decades, halogenated compounds have been widely used in the economical reduction of polymer

flammability without compromising product quality. However, halogen-based fire retardants have been found to have negative environmental effects due to their toxicity and persistence in the environment.<sup>6–8</sup> Because of these undesirable features, great strides have been made in the search for alternative fire retardants. At the moment, inorganic nanofillers represents the most predominant route nanotechnology can produce PMCs with flame retarding properties. In particular, modified and unmodified layered silicates are undoubtedly the most widely used nanofillers that serve as flame retardants. In addition to the extensively researched organoclays, other nanofillers such as; graphene and graphene oxide,<sup>9,10</sup> polyhedral oligomeric silsesquioxanes (POSS),<sup>11,12</sup> layered double hydroxides (LDH),<sup>13</sup> nanosilica,<sup>14</sup> metal oxides, and recently, metal-organic frameworks<sup>15,16</sup> are also generating a lot of interest in fire research. It is highly desirable to produce PMCs that have markedly enhanced thermal resistance and improved flammability properties when only small amounts of the nanofillers are loaded so that desirable physical

\*For correspondence

properties of the polymer matrix are not compromised. Hence the thermal resistance of polymer hosts should be markedly enhanced when a small amount of nanofillers is loaded. Polystyrene (PS) is a well-known thermoplastic polymer widely used for various applications<sup>17</sup> because it is cheap, has very good chemical resistance, low density, very good thermal and electrical insulation and is easy to process.<sup>5,18</sup> Despite all these very good properties, the high flammability of styrene-based materials limits their wider uses. When styrene-based polymers are exposed to elevated temperatures, they easily depolymerize releasing numerous volatile products such as styrene monomers, dimers, trimers, and other hydrocarbons.<sup>15,16</sup> In the last decade, a lot of work has been done to develop environmentally-friendly fire-retardant formulations that have been shown to be effective for PS.<sup>5,16,19–23</sup> Among the proposed fire-retardant solutions, compounds containing phosphorus (P) atom(s) have been shown to be highly effective<sup>24,25</sup> with phosphorus acting in the condensed or gas phase depending on the valence.<sup>26</sup> Phosphorus-containing compounds are also considered to be less toxic than the corresponding halogen-containing formulations.<sup>27,28</sup> Despite a lot of phosphorous-containing formulations developed to reduce the flammability of common household and everyday use polymers, it is still challenging to design non-toxic, environmentally friendly yet efficient fire retardants for polystyrene. The purpose of this work was to investigate the potential of using aluminum and silicon phosphates as nanofillers in polystyrene to improve its fire properties. Inorganic phosphates are of interest in various applications as they exhibit interesting technological and structural properties. A particular feature of the alkali and alkali-earth phosphosilicate glasses is that a fraction of the  $\text{Si}^{4+}$  ions is octahedrally coordinated as seen in  $\text{Si}_5\text{O}(\text{PO}_4)_6$ ,  $\text{Si}_3(\text{PO}_4)_4$  and  $\text{SiP}_2\text{O}_7$ . The silicon phosphates are the only normal pressure ionic crystalline phases known to have  $\text{SiO}_6$  units. Because of these unique properties, silicon phosphate particles have a very large interfacial area which promotes tight packing when mixed with polymers and consequently has the potential of improving fire and mechanical properties in composites. Aluminum phosphates are of interest due to their good thermal stability and surface acidity which can promote char formation during polymer decomposition. Silicon and Aluminum phosphates have been synthesized in a variety of ways depending on the particular application, with specialized applications requiring adverse conditions of pressure and temperature.<sup>29–33</sup> Herein we report the potential of  $\text{AlPO}_4$ ,  $\text{Si}_5\text{O}(\text{PO}_4)_6$  and  $\text{K}_3\text{Al}_5((\text{PO}_4)_2(\text{HPO}_4))_6 \cdot x\text{H}_2\text{O}$  prepared

by sol-gel synthetic methods as viable alternative fire retardants for polystyrene.

## 2. Experimental

### 2.1 Preparation of aluminum and silicon phosphate

Crystalline silicon phosphate ( $\text{Si}_5\text{O}(\text{PO}_4)_6$ ) was synthesized using 85%  $\text{H}_3\text{PO}_4$  (JT Baker, USA) and silica gel (Sigma Aldrich, USA) as sources of phosphorous and silicon, respectively. Initially,  $\text{H}_3\text{PO}_4$  was heated to 140 °C for 1 h and then silica gel was slowly added to the acid. The ratio Si:P in the reaction mixture was 1:3 by mass. The reaction mixture was then refluxed at 200 °C for 6 h. The product was washed thoroughly with deionized water followed by acetone and then dried at 100 °C for 2 hours followed by calcination at 800 °C for 2 h.

$\text{AlPO}_4$  was synthesized from 85%  $\text{H}_3\text{PO}_4$  and sodium aluminate (Strem Chemicals, USA). 5 g of sodium aluminate was added to 100 mL of 2-butanol followed by heating to 100 °C. Thereafter 20 mL of concentrated  $\text{H}_3\text{PO}_4$  was added drop wise with stirring followed by refluxing at 100 °C for 24 h. The white precipitate was washed with water and ethanol and dried at 80 °C for 6 h.

For  $\text{K}_3\text{Al}_5((\text{PO}_4)_2(\text{HPO}_4))_6 \cdot x\text{H}_2\text{O}$  synthesis, 100 mL of a 0.12 M solution of  $\text{Al}(\text{NO}_3)_3 \cdot 9\text{H}_2\text{O}$  in previously boiled deionized water was added drop wise with stirring to a 180 mL solution of 0.24 M ( $\text{KOH} + \text{KH}_2\text{PO}_4$ ). After ageing for 24 h at room temperature under constant stirring, the slurry was washed thoroughly with deionized and decarbonated water then finally air-dried at room temperature. The aluminum phosphate synthesized using this method was identified as taranakite.

### 2.2 Preparation of polystyrene composites

Polystyrene ( $M_w$  ca. 192 000; melt index 6.0–9.0 g per 10 min, 200 °C/5 kg; purchased from Sigma Aldrich, USA) composites were prepared *via* melt blending in a Brabender Plasticoder. The Brabender Plasticoder melt blending operational parameters are; temperature = 200 °C, screw speed = 60 rpm, and residence time = 10 min. The constituent components of the different composite samples are presented in Table 1. Entry 1 (PS), in Table 1, represents the polystyrene reference sample, without any additive, that was subjected to the same procedure as the composites.

**Table 1.** Composition of polystyrene composites.

	Sample name	Polystyrene PS (%)	AIP (%)	SiP (%)	Taranakite (%)
1	PS	100	0	0	0
2	PS-2AIP	98	2	0	0
3	PS-5AIP	95	5	0	0
4	PS-10AIP	90	10	0	0
5	PS-2SiP	98	0	2	0
6	PS-5SiP	95	0	5	0
7	PS-10SiP	90	0	10	0
8	PS-2taranakite	98	0	0	2
9	PS-5taranakite	95	0	0	5
10	PS-10taranakite	90	0	0	10

### 2.3 Characterization

Powder X-ray diffraction (PXRD) patterns ( $2\theta$  range of  $2.0\text{--}80.0^\circ$ ; step size of  $0.083^\circ$  per second) were obtained on a Rigaku Miniflex II X-ray diffractometer (USA) utilizing Cu ( $K\alpha$ ) X-ray source of wavelength of  $1.54 \text{ \AA}$ , 30 kV generating voltage and 15 mA current. Powdered samples were mounted onto quartz slides while polymer samples were pressed into platelets and mounted on aluminum sample holders. Attenuated total reflectance-Fourier transform infrared (ATR-FTIR) spectra of the synthesized materials and the composites were obtained on a Perkin Elmer Spectrum 100 FTIR spectrometer, USA. The ATR-FTIR spectrometer was operated at  $2 \text{ cm}^{-1}$  resolution and  $4000\text{--}650 \text{ cm}^{-1}$  spectral range utilizing a MIRacle™ single reflection ATR accessory from PIKE Technologies. Thermogravimetric (TG) data was obtained on a NETZSCH TG 209 F1 (Germany) instrument using ceramic sample holders. The temperature range was 30 to  $500 \text{ }^\circ\text{C}$  at a ramp rate of  $20 \text{ K min}^{-1}$  in an inert  $\text{N}_2$  (flow rate of  $50 \text{ mL min}^{-1}$ ) atmosphere. Triplicate measurements were recorded, and the average was reported here. An Atlas Cone 2 instrument (USA) was used to evaluate the flammability of the pure polymer and its composites. For the cone calorimetry analysis, the samples weighing about 30 g and of the dimensions  $100 \text{ mm} \times 100 \text{ mm} \times 3 \text{ mm}$  were subjected to an incident heat flux of  $35 \text{ kW m}^{-2}$  in a horizontal orientation. The analysis was conducted in triplicates and the reported values are the averages of three measurements.

## 3. Results and Discussion

### 3.1 Characterization of materials

Powder X-ray diffraction (PXRD) patterns of silicon and aluminum phosphate samples are shown in Figure 1. The  $d$  spacings and the relative intensities

of the samples match well with the corresponding values reported for  $\text{K}_3\text{Al}_5((\text{PO}_4)_2(\text{HPO}_4)_6 \cdot x\text{H}_2\text{O})$ , silicon orthophosphate  $\text{Si}_5\text{O}(\text{PO}_4)_6$  and  $\text{AlPO}_4$ .

The nature of the inorganic filler-polymer composites can also be evaluated by XRD. For layered materials, the intercalation of the polymer matrix within the interlayer space results in an increase in the interlayer spacing of the resultant composite material that is detected as a shift of Bragg reflections to lower  $2\theta$  values on the XRD pattern. An exfoliated system results from the complete loss of the layered structure with the individual layers dispersed within the polymer matrix leading to complete loss of registry between the layers such that no Bragg reflections are observed. However, various types of disorders can lead to loss of peaks on the XRD traces therefore the absence of peaks is not proof of exfoliation. Figure 2 shows representative XRD patterns of PS and its composites. For PS-taranakite composites, there appear to be a loss

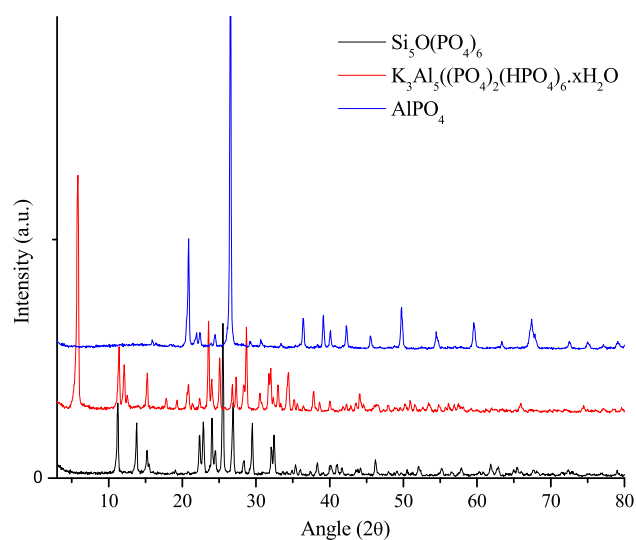


**Figure 1.** Powder X-ray diffraction traces for  $\text{Si}_5\text{O}(\text{PO}_4)_6$ ,  $\text{K}_3\text{Al}_5((\text{PO}_4)_2(\text{HPO}_4)_6 \cdot x\text{H}_2\text{O})$  and  $\text{AlPO}_4$ .

in crystallinity of taranakite when it is mixed with polystyrene. This may suggest that taranakite might have become disordered when it was blended with PS at an elevated temperature. Temperature-dependent XRD studies have shown that at temperatures greater than 200 °C, taranakite transforms into an amorphous phase,<sup>34</sup> which support our suggestion rather than masking of the taranakite peaks by the large amorphous hump from PS. For  $\text{Si}_5\text{O}(\text{PO}_4)_6$  and  $\text{AlPO}_4$  composites, there are small sharp peaks in addition to the broad PS peaks indicating that the crystalline structures were maintained, but were masked by the big amorphous PS hump.

FTIR results of silicon and aluminum phosphates are shown in Figure 3. The phosphate  $\nu_3$  and  $\nu_1$  bands for aluminum phosphate and taranakite are identified by three peaks (1087, 1042, and 911  $\text{cm}^{-1}$ ).<sup>35</sup> For silicon orthophosphate, the phosphate  $\nu_3$  and  $\nu_1$  bands appear at 1163, 1101 and 1023  $\text{cm}^{-1}$ .

### 3.2 Thermal stability

To investigate the individual temperature-dependent transformations which the additives undergo before being incorporated into polystyrene, thermogravimetric analysis was conducted, and the results are presented in Figure 4. The loss of physically adsorbed and chemically bound water manifests as the weight loss below 200 °C, and the losses at  $T > 200$  °C can be assigned to the decomposition of the phosphates.<sup>36,37</sup> Even though the mechanisms of mass loss are different in  $\text{AlPO}_4$  and

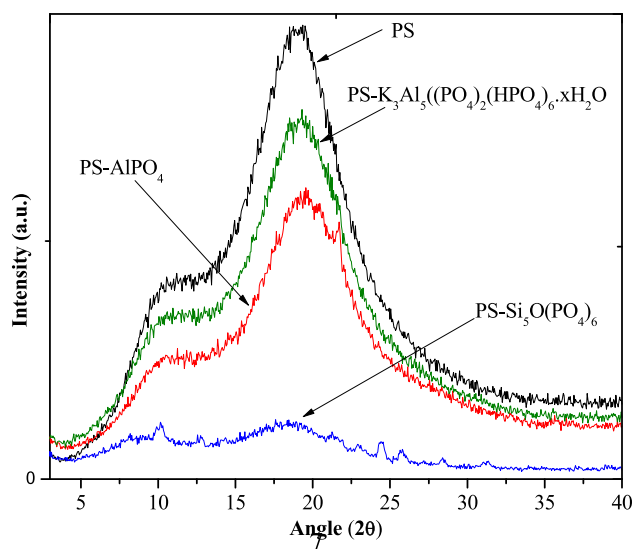


**Figure 2.** Powder X-ray diffraction data for pure polystyrene,  $\text{Si}_5\text{O}(\text{PO}_4)_6$ ,  $\text{K}_3\text{Al}_5((\text{PO}_4)_2(\text{HPO}_4)_6 \cdot x\text{H}_2\text{O})$  and  $\text{AlPO}_4$ -polystyrene composites.

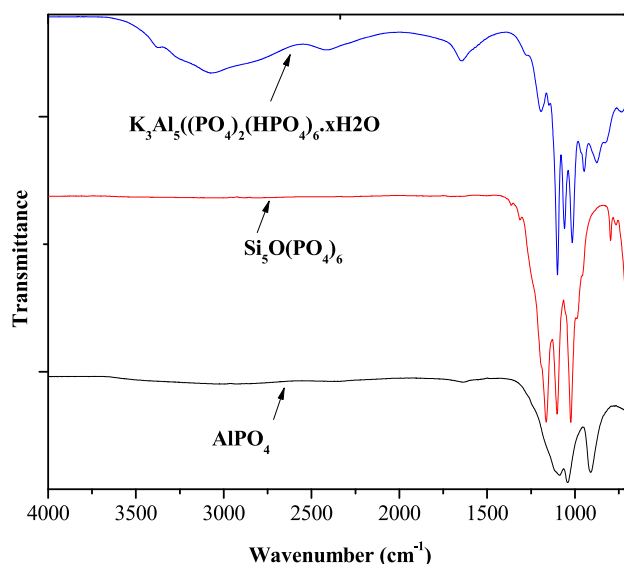


**Figure 3.** FTIR traces for  $\text{Si}_5\text{O}(\text{PO}_4)_6$ ,  $\text{K}_3\text{Al}_5((\text{PO}_4)_2(\text{HPO}_4)_6 \cdot x\text{H}_2\text{O})$  and  $\text{AlPO}_4$ . Traces are offset for clarity but not otherwise scaled.

$\text{Si}_5\text{O}(\text{PO}_4)_6$  as evidenced by different TGA profiles, the percentage weight loss after heating to 800 °C is the same.  $\text{AlPO}_4$  and  $\text{Si}_5\text{O}(\text{PO}_4)_6$  additives lose about 14% of their starting weight whereas  $\text{K}_3\text{Al}_5((\text{PO}_4)_2(\text{HPO}_4)_6 \cdot x\text{H}_2\text{O})$  loses about 25% of its weight when heated to 800 °C.

The temperature dependent mass loss data obtainable from TGA has led to the technique being routinely used to compare the thermal stability of pure polymers and polymer composites. Improvements in thermal stability of the composites, bestowed by the inorganic fillers, were evaluated making use of TGA data presented in Figure 5. The onset of thermal degradation (which we consider as the temperature at

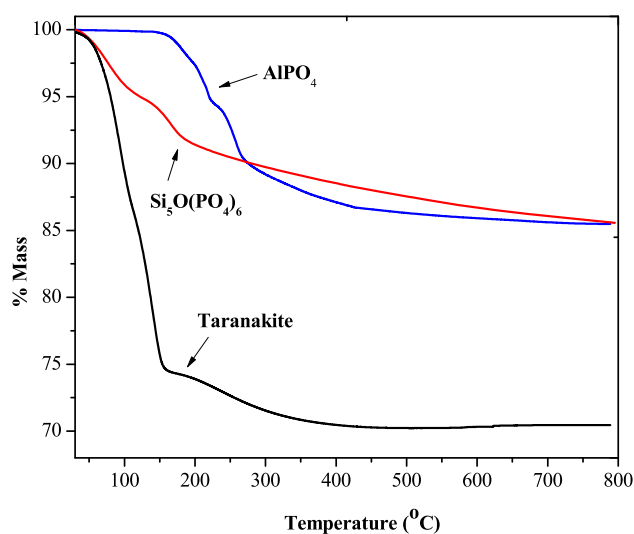


**Figure 4.** TGA curves of  $\text{K}_3\text{Al}_5((\text{PO}_4)_2(\text{HPO}_4)_6 \cdot x\text{H}_2\text{O})$ ,  $\text{Si}_5\text{O}(\text{PO}_4)_6$  and  $\text{AlPO}_4$ .

which 10% mass loss occurs,  $T_{0.1}$ ) of pure polystyrene is 378 °C. The onset of degradation in PS–AIP composites increases by less than 10 °C when compared to the unmodified polymer at all three different loading levels. Mid-point temperature (the temperature at which 50% mass loss occurs,  $T_{0.5}$ ) also showed the same trend as the onset degradation temperature. For the PS– $\text{Si}_5\text{O}(\text{PO}_4)_6$  composites, onset degradation temperature increases by between 9 and 27 °C and  $T_{0.5}$  increases by between 13 and 31 °C. The increases in  $\text{Si}_5\text{O}(\text{PO}_4)_6$  containing samples is dependent on additive loading percentage, with a high loading giving more thermal stability. Phosphates have been shown to act in the condensed phase by enhancing surface char formation during polymer composites decomposition.<sup>38</sup> The surface char acts as a barrier to mass and heat transfer restricting the passage of polymer matrix degradation products. The key properties obtained from thermogravimetry analysis are summarized in Table 2.

Results summarized in Table 2 indicate the following order of thermal stability for the nanocomposites under investigation: PS–SiP>PS–AIP>PS–taranakite. This order correlates well with the char formation capabilities of the additives. Silicon and phosphorus have been shown to have a char forming synergy with phosphorus enhancing char formation whilst silicon protects the char from degrading.<sup>39</sup> Flame retardants containing Si and P have been shown to form crosslinking residues which have excellent flame and smoke suppression effects.<sup>40</sup>

### 3.3 Evaluation of flammability

The effects of the additives on the flammability of PS were investigated using cone calorimetry.

The cone calorimeter is one of the main instruments that are widely used in the evaluation of the effectiveness of additives as flame retardants. The utility of the

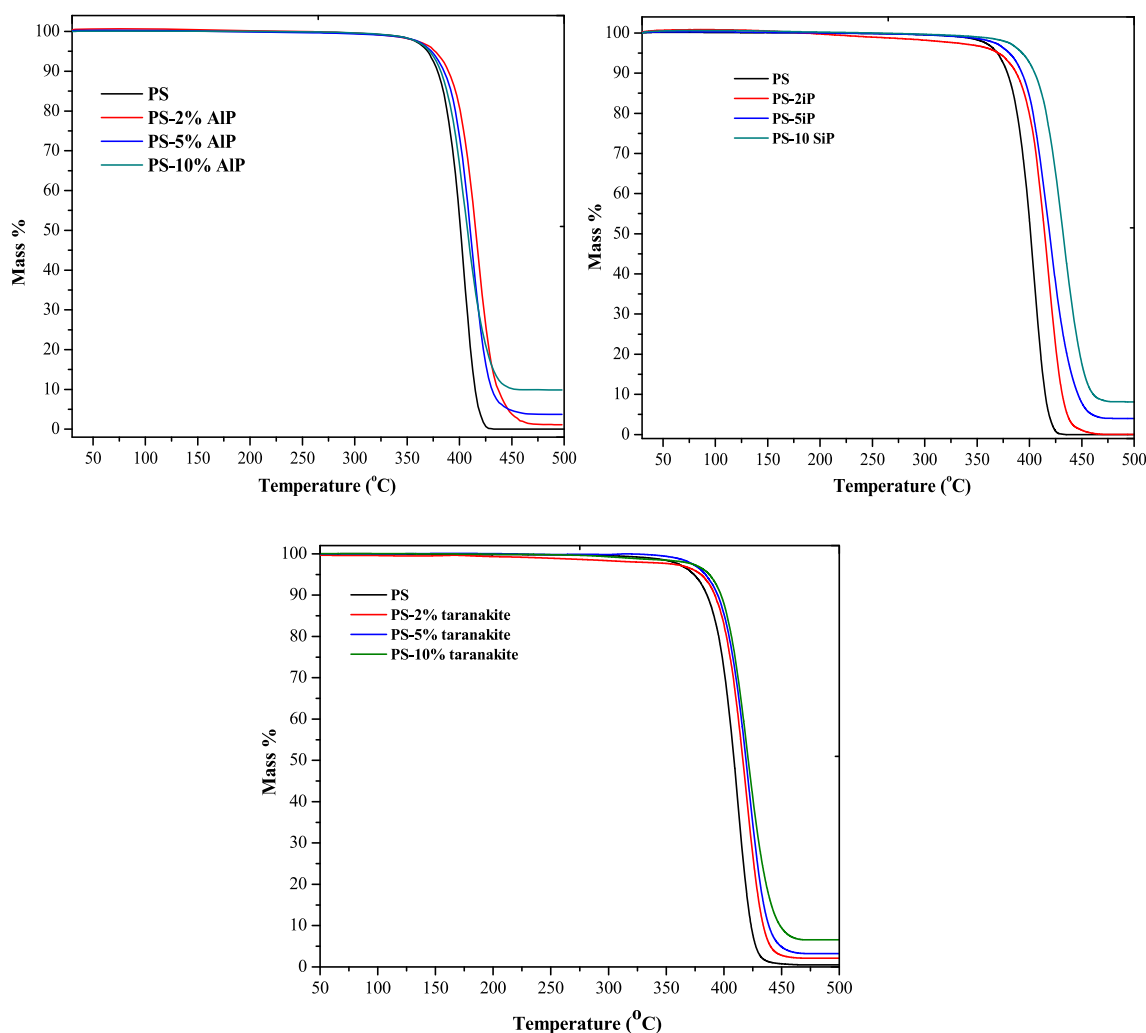


**Figure 5.** TGA curves for neat PS, PS– $\text{AlPO}_4$ , PS– $\text{Si}_5\text{O}(\text{PO}_4)_6$  and PS– $\text{K}_3\text{Al}_5((\text{PO}_4)_2(\text{HPO}_4)_6 \cdot x\text{H}_2\text{O})$ .

**Table 2.** TGA data for pure polystyrene and its composites.

Sample	T <sub>0.1</sub> (°C)	T <sub>0.5</sub> (°C)	ΔT <sub>0.5</sub>	% Char
PS	378±1	401±2	-	0.2±0.1
PS-2AIP	386±2	411±2	10±1	1.7±0.3
PS-5AIP	387±3	413±1	12±2	4.6±0.4
PS-10AIP	388±2	412±0	11±1	10.1±0.6
PS-2SiP	387±3	414±2	13±1	1.7±0.5
PS-5SiP	393±2	419±3	18±2	4.8±0.8
PS-10SiP	405±2	432±2	31±3	10.6±0.9
PS-2 taranakite	386±2	407±2	4±2	1.7±0.2
PS-5 taranakite	388±3	409±5	8±2	4.2±0.4
PS-10 taranakite	390±2	414±3	13±3	7.6±1.2

ΔT<sub>0.5</sub>; T<sub>0.5</sub> (composite) minus T<sub>0.5</sub> (pure PS). Italicized entries are the expected char based on the residue obtained from pure PS and additive fractions

cone calorimeter stems from the obtained parameters such as heat release rate (HRR), peak of HRR (PHRR), total heat release (THR), smoke production (ASEA), average mass loss rate (AMLR) and time to ignition, (*t<sub>ig</sub>*), which are key in assessing the flammability of materials. An ideal additive should cause significant decreases in PHRR, THR, ASEA and AMLR while increasing the time to ignition. To simulate radiant heat during fire development, a heat flux of 35 kW/m<sup>2</sup> was used in the cone calorimetry experiments<sup>41</sup> and the results from the experiments are shown in Figure 6. The HRR results shown in Figure 6 show that the HRR traces for the composites span a wider time interval compared to the pure polymer which indicates that the composite materials burn for a longer time compared to the pure PS. THR values, which are obtained from the integration of the HRR curves, provide an indication of the extent of the burning of the pure polymer or the polymer matrix in the composite. Results presented in Table 3 show that THR values of the composites are within the experimental error margins of the neat polymer. This indicates that the additives did not significantly reduce the extent of burning of the polymer matrix within the composite and the polymer completely decomposed at the end of the cone calorimetry experiment.

There was a decrease in smoke production with increasing additive loading, the best results were obtained at 10% Si<sub>5</sub>O(PO<sub>4</sub>)<sub>6</sub> loading which caused a 13% reduction in ASEA. AMLR decreased slightly at higher additive loadings with the greater reduction being observed for Si<sub>5</sub>O(PO<sub>4</sub>)<sub>6</sub> as compared to AlPO<sub>4</sub> and taranakite. As previously observed for most inorganic fillers, the time to sustained ignition is reduced for all the composites. This has been attributed to the increase in polymer viscosity due to

the addition of the fillers, which reduce the heat exchange between the surface of the sample exposed to heat flux and the bulk polymer matrix.<sup>42</sup> This results in a rapid increase in the surface temperature which reduces the time required for the sample to reach pyrolysis temperature.<sup>43</sup> The results presented in Figure 6 and summarized in Tables 3 and 4 highlight the effects of the additives in reducing the peak heat release rate, with a substantial reduction of 52% being observed for PS-10SiP. Table 4 shows that the addition of Si<sub>5</sub>O(PO<sub>4</sub>)<sub>6</sub> led to the best improvements in the fire properties when compared to other modifiers. Figure 5 shows that polystyrene degrades in a single step in the temperature range 300 to 500 °C. This degradation has been shown to occur *via* statistical β-scission of the polystyrene backbone.<sup>42</sup> The external heat flux initiates the degradation process, releasing volatile molecules (styrene, α-methyl styrene, benzene, and toluene) which release substantial amounts of energy upon oxidation. The heat released due to the oxidation of these volatile degradation products is fed to the bulk composite causing further degradation of the polymer matrix resulting in the release of more volatile degradation products which are then oxidized releasing more heat. This creates a cycle (burning cycle) that is responsible for sustaining the burning process after the removal of the external heat source. Effective fire retardants act by breaking this burning cycle through improving the thermal stability of the polymer, dilution and consequent quenching of the flame, and formation of a heat and mass transfer barrier.<sup>44</sup> Si<sub>5</sub>O(PO<sub>4</sub>)<sub>6</sub>, taranakite, and AlPO<sub>4</sub> might act as “heat shields” which may limit heat feedback to the bulk polymer by reducing heat conduction into polystyrene. They can also limit gas evolved due to an increase in melt viscosity and can also enhance the wetting of mineral particles by the molten polymer. Unlike organic phosphorus compounds which can act both in the condensed phase and in the gas phase, inorganic compounds mainly act in the condensed phase catalyzing char formation.<sup>22,38,45</sup> Therefore, the formation of a continuous char that act as an efficient barrier to heat and mass transfer is critical for an effective flame retardant as it screens degradation products below the heated surface from the burning fire. Therefore additives that form continuous char act as better flame retardants than aggregates and pillars forming additives.<sup>46</sup>

Photographs of char formed from PS and its composites after the cone calorimetry tests shown in Figure 7 indicates that the appearance of the char differed depending upon the additives. Residual char

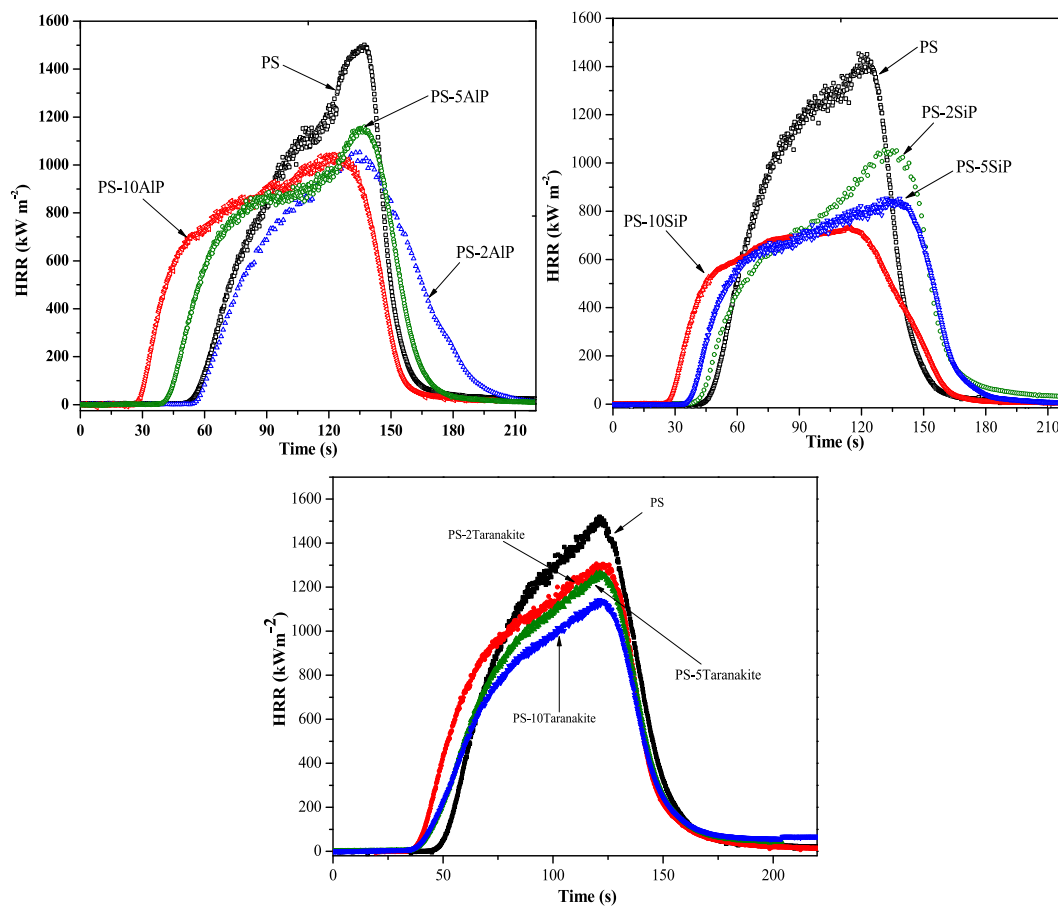


**Figure 6.** Heat release curves for neat PS, PS-  $K_3Al_5((PO_4)_2(HPO_4)_6 \cdot xH_2O)$ , PS- $AlPO_4$  and PS- $Si_5O(PO_4)_6$ .

**Table 3.** Cone calorimetry data for PS composites at  $35 \text{ kW m}^{-2}$ .

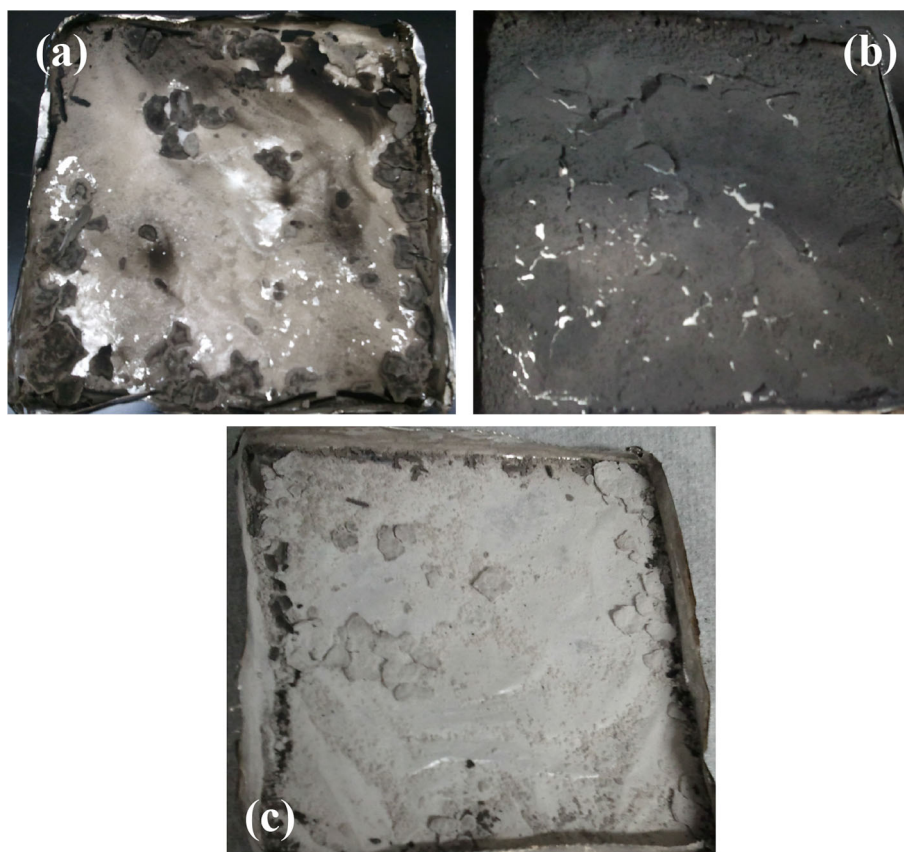
Sample	$t_{ign}(s)$	PHRR ( $\text{kW m}^{-2}$ ) (% reduction)	$t_{PHRR}(s)$	THR ( $\text{MJ m}^{-2}$ )	AMLR ( $\text{g sec m}^{-2}$ )	ASEA ( $\text{m}^2 \text{ kg}^{-1}$ )
PS	43±1	1489±56	142±6	94±4	30±2	1356±87
PS-2AIP	38±2	1346±43	142±4	88±3	26±3	1280±65
PS-5AIP	31±3	1243±34	140±3	89±6	29±3	1270±46
PS-10AIP	28±3	1165±58	138±5	88±3	25±3	1256±39
PS-2SiP	34±2	990±29	148±6	87±3	24±1	1218±25
PS-5SiP	32±2	840±15	149±7	83±4	23±2	1204±19
PS-10SiP	25±3	722±18	126±5	81±4	20±1	1178±33
PS-2 taranakite	28±2	1412±65	141±7	93±9	25±2	1343±21
PS-5 taranakite	26±1	1342±47	140±8	111±5	25±2	1295±47
PS-10 taranakite	10±1	1168±51	139±5	102±5	27±1	1270±24

from the PS-AIP (a) and PS-taranikite (c), formed multiple islands with discontinuities that occupy a small area relative to the original sample area. The synergistic effects of silicon and phosphorus<sup>39</sup> resulted in the char from PS-SiP (Figure 7b) being firm, intact and uniformly distributed occupying close to 100% of the original sample area.

$Si_5O(PO_4)_6$  containing formulations were more effective in reducing flammability when compared to other formulations due to the highly dense char network that was impermeable to gases, hence providing a barrier to diffusion of volatile degradation products to the pyrolysis zone thereby retarding the combustion process.<sup>46,47</sup>

**Table 4.** Comparison of different modifiers on fire properties of polystyrene.

Additive	Loading (%)	PHRR Reduction (%)	THR	ASEA Change (%)	AMLR	Reference
Si <sub>5</sub> O(PO <sub>4</sub> ) <sub>6</sub>	10	52	81±4	-13	20±1	This work
AlPO <sub>4</sub>	10	22	88±3	-7	25±3	This work
Taranakite	10	22	102±5	-6	27±1	This work
MgAl-undecenoate/APP	5/5	42	101±1		16±1	<a href="#">42</a>
Organically modified MMT (various modifiers)	5	16-37	86-94	+3 to +15	24-27	<a href="#">44</a>
DOPO	23	17	64.9	-	-	<a href="#">22</a>
Graphene oxide functionalized DOPO	23	28	62.8	-	-	<a href="#">22</a>
Bis(2,4-dicumylphenyl) pentaerythritol diphosphate	10	22	101	-61	-	<a href="#">38</a>
Sugar beet leaves derived graphite sheets	10	28	110±8	-26	-	<a href="#">10</a>
Graphitic carbon nitride/organic aluminum hypophosphites	4	27	89.0	-17	-	<a href="#">20</a>

**Figure 7.** Photographs of residual char (a) PS-5% AlPO<sub>4</sub> (b) PS-5% Si<sub>5</sub>O(PO<sub>4</sub>)<sub>6</sub> (c) PS-K<sub>3</sub>Al<sub>5</sub>((PO<sub>4</sub>)<sub>2</sub>(HPO<sub>4</sub>)<sub>6</sub>·xH<sub>2</sub>O.

#### 4. Conclusions

Polystyrene composites containing K<sub>3</sub>Al<sub>5</sub>((PO<sub>4</sub>)<sub>2</sub>(HPO<sub>4</sub>)<sub>6</sub>·xH<sub>2</sub>O, Si<sub>5</sub>O(PO<sub>4</sub>)<sub>6</sub> and AlPO<sub>4</sub> were prepared via melt blending and characterized by XRD, FTIR and cone calorimetry. Thermo-gravimetric analysis revealed that addition of AlPO<sub>4</sub> caused small increases

in thermal stability as evidenced by approximately a 7 °C increase in onset degradation temperature and approximately an 11 °C increase in the midpoint degradation temperature. The addition of Si<sub>5</sub>O(PO<sub>4</sub>)<sub>6</sub> caused increases between 9 and 27 °C in the onset degradation temperature and between 13 and 31 °C in the midpoint degradation temperature. Thermal

stability increases due to  $\text{AlPO}_4$  was independent of percentage loading whilst that from  $\text{Si}_5\text{O}(\text{PO}_4)_6$  was directly proportional to loading. The addition of  $\text{Si}_5\text{O}(\text{PO}_4)_6$  and the aluminum phosphates at loadings of no more than 10% resulted in substantial reductions in peak heat release rate (PHRR) as determined from cone calorimetry.  $\text{Si}_5\text{O}(\text{PO}_4)_6$  additive resulted in the greatest reduction in the PHRR of PS as compared to the other additives. This was mainly due to the  $\text{Si}_5\text{O}(\text{PO}_4)_6$  forming a more compact char during the burning process. Similar reductions were observed for the average mass loss rate (AMLR) suggesting that reductions in PHRR are due to the slower rate at which combustible volatiles are produced. Between the phosphates investigated  $\text{Si}_5\text{O}(\text{PO}_4)_6$  gave the best results.

### Acknowledgements

We would like to thank the department of chemistry at Marquette University for the use of the cone calorimeter.

**Conflict of interest** The authors declare that they have no conflicts of interest.

### References

- Kiliaris P and Papaspyrides C D 2010 Polymer/layered silicate (clay) nanocomposites: An overview of flame retardancy *Prog. Polym. Sci.* **35** 902
- Beyer G 2002 Nanocomposites: A new class of flame retardants for polymers *Plast. Addit. Compd.* **4** 22
- Lu S Y and Hamerton I 2002 Recent developments in the chemistry of halogen-free flame retardant polymers *Prog. Polym. Sci.* **27** 1661
- Zhu Z M, Xu Y J, Liao W, Xu S and Wang Y Z 2017 Highly flame retardant expanded polystyrene foams from phosphorus-nitrogen-silicon synergistic adhesives *Ind. Eng. Chem. Res.* **56** 4649
- Shao X, Du Y, Zheng X, Wang J, Wang Y, Zhao S, et al. 2020 Reduced fire hazards of expandable polystyrene building materials via intumescent flame-retardant coatings *J. Mater. Sci.* **55** 7555
- Aminot Y, Lanctôt C, Bednarz V, Robson W J, Taylor A, Ferrier-Pagès C, et al. 2020 Leaching of flame-retardants from polystyrene debris: Bioaccumulation and potential effects on coral *Mar. Pollut. Bull.* **151** 110862
- Mekni S, Barhoumi B, Touil S, Driss M R and Eljarrat E 2020 Occurrence of halogenated and organophosphate flame retardants in sediments and eels (*Anguilla anguilla*) from Bizerte Lagoon, Tunisia *Front. Environ. Sci.* **8** 67
- Hsu Y C, Arcega R A D, Gou Y Y, Tayo L L, Lin Y H, Lin S H and Chao H R 2018 Levels of non-PBDE halogenated fire retardants and brominated dioxins and their toxicological effects in indoor environments-A review *Aerosol. Air Qual. Res.* **18** 2047
- Sabet M, Soleimani H, Mohammadian E and Hosseini S 2020 The effect of graphene oxide on flame retardancy of polypropylene and polystyrene *Mater. Perform. Charact.* **9** 284
- Attia N F 2021 Sustainable and efficient flame retardant materials for achieving high fire safety for polystyrene composites *J. Therm. Anal. Calorim.* <https://doi.org/10.1007/s10973-021-10948-3>.
- Yu B, Yuen A C Y, Xu X, Zhang Z C, Yang W, Lu H, et al. 2020 Engineering MXene surface with POSS for reducing fire hazards of polystyrene with enhanced thermal stability *J. Hazard. Mater.* **401** 123342
- Guo Y, Cui J, Guo J, Zhang H, Wang L and Yang B 2020 Modification of POSS hybrids by ionic liquid simultaneously prolonging time to ignition and improving flame retardancy for polystyrene *J. Polym. Res.* **27** 101
- Manzi-nshuti C, Wang D, Hossenlopp J H and Wilkie C A 2008 Aluminum-containing Layered Double Hydroxides: the Thermal, Mechanical, and Fire Properties of (Nano) composites of Poly (methyl Methacrylate) *J. Mater Chem.* **18** 3091
- Ahmed L, Zhang B, Shen R, Agnew R J, Park H, Cheng Z, et al. 2018 Fire reaction properties of polystyrene-based nanocomposites using nanosilica and nanoclay as additives in cone calorimeter test *J. Therm. Anal. Calorim.* **132** 1853
- Xu Z, Xing W, Hou Y, Zou B, Han L, Hu W and Hu Y 2021 The combustion and pyrolysis process of flame-retardant polystyrene/cobalt-based metal organic frameworks (MOF) nanocomposite *Combust. Flame.* **226** 108
- Zhang J, Li Z, Qi X L and Wang D Y 2020 Recent Progress on Metal-Organic Framework and Its Derivatives as Novel Fire Retardants to Polymeric Materials *Nano-Micro Lett.* **12** 173
- Sulong N H R, Mustapa S A S and Rashid M K A 2019 Application of expanded polystyrene (EPS) in buildings and constructions: A review *J. Appl. Polym. Sci.* **136** 47529
- Lynwood C 2014 *Polystyrene: Synthesis, Characteristics, and Applications* (New York: Nova Science Publishers)
- Hou Y, Hu W, Gui Z and Hu Y 2017 Preparation of Metal-Organic Frameworks and Their Application as Flame Retardants for Polystyrene *Ind. Eng. Chem. Res.* **56** 2036
- Shi Y, Yu B, Duan L, Gui Z, Wang B, Hu Y and Yuen R K K 2017 Graphitic carbon nitride/phosphorus-rich aluminum phosphinates hybrids as smoke suppressants and flame retardants for polystyrene *J. Hazard Mater.* **332** 87
- Mountassir A, Tirri T, Sund P and Wilén C E 2021 Sulfenamides as Standalone Flame Retardants for Polystyrene *Polym. Degrad. Stab.* **188** 109588
- Li L, Shao X, Zhao Z, Liu X, Jiang L, Huang K and Zhao S 2020 Synergistic Fire Hazard Effect of a Multifunctional Flame Retardant in Building Insulation Expandable Polystyrene through a Simple Surface-Coating Method *ACS Omega* **5** 799
- Huang J, Zhao Z Q, Chen T, Zhu Y, Lv Z H, Gong X, et al. 2019 Preparation of highly dispersed expandable graphite/polystyrene composite foam via suspension

- polymerization non-covalently compatibilized by polystyrene with enhanced fire retardation *Carbon* **146** 503
24. Qian X, Zheng K, Lu L, Wang X and Wang H 2018 A novel flame retardant containing calixarene and DOPO structures: Preparation and its application on the fire safety of polystyrene *Polym. Adv. Technol.* **29** 2715
  25. Wang J, Yuan B, Cai W, Qiu S, Tai Q, Yang H and Hu Y 2018 Facile design of transition metal based organophosphorus hybrids towards the flame retardancy reinforcement and toxic effluent elimination of polystyrene *Mater. Chem. Phys.* **214** 209
  26. Chen M-J, Xu Y-J, Rao W-H, Huang J-Q, Wang X-L, Chen L and Wang Y-Z 2014 Influence of valence and structure of phosphorus-containing melamine salts on the decomposition and fire behaviors of flexible polyurethane foams *Ind. Eng. Chem. Res.* **53** 8773
  27. Benin V, Cui X, Morgan A B and Seiwert K 2015 Synthesis and flammability testing of epoxy functionalized phosphorous-based flame retardants *J. Appl. Polym. Sci.* **132** 42296
  28. Morgan A B 2019 The Future of Flame Retardant Polymers-Unmet Needs and Likely New Approaches *Polym. Rev.* **59** 25
  29. Styskalik A, Skoda D, Moravec Z, Roupцова P, Barnes C E and Pinkas J 2015 mesoporous nanocrystalline silicon *RCS Adv.* **5** 73670
  30. Wu Z, Guo G, Hu L and Chen H 2020 Synthesis and Characterization of Ultrafine Aluminum Phosphate Powder in CTAB System *IOP Conf. Ser.: Mater. Sci. Eng.* 746
  31. Devamani R H P and Alagar M 2012 Synthesis and Characterization of Aluminium Phosphate Nanoparticles *Int. J. Appl. Sci. Eng. Res.* **1** 769
  32. Lagno F and Demopoulos G P 2005 Synthesis of hydrated aluminum phosphate,  $\text{AlPO}_4 \cdot 1.5\text{H}_2\text{O}$  ( $\text{AlPO}_4\text{-H}_3$ ), by controlled reactive crystallization in sulfate media *Ind. Eng. Chem. Res.* **44** 8033
  33. Leinenweber K, Stearns L A, Nite J M, Németh P and Groy T L 2012 Structure of a new form of silicon phosphate ( $\text{SiP}_2\text{O}_7$ ) synthesized at high pressures and temperatures *J. Solid State Chem.* **190** 221
  34. Wang N 2009 Flame Retardancy of Polymer Nanocomposites based on Layered Aluminum Phosphate and Computational Study of Intercalation of Amines into  $\alpha$ -Zirconium Phosphate and Adsorption of a Model Organic Pollutant. Published online 2009. [http://epublications.marquette.edu/theses\\_open/120](http://epublications.marquette.edu/theses_open/120)
  35. Gibson I R, Best S M and Bonfield W 1999 Chemical characterization of silicon-substituted hydroxyapatite *J. Biomed. Mater. Res.* **44** 422
  36. Bamzai K K, Kachroo N, Singh V and Verma S 2013 Synthesis, Characterization, and Thermal Decomposition of Pure and Dysprosium Doped Yttrium Phosphate System *J. Mater.* **2013** 359514
  37. Liu H, Zhang B and Han J 2017 Flame retardancy and smoke suppression properties of flexible polyurethane foams containing an aluminum phosphate microcapsule *RSC Adv.* **7** 35320
  38. Majoni S 2015 Thermal and flammability study of polystyrene composites containing magnesium – aluminum layered double hydroxide (MgAl – C16 LDH), and an organophosphate *J. Therm. Anal. Calorim.* **20** 1435
  39. Wang X, Hu Y, Song L, Xing W and Lu H 2010 Thermal Degradation Behaviors of Epoxy Resin/POSS Hybrids and Phosphorus – Silicon Synergism of Flame Retardancy *J. Polym. Sci. Part B Polym. Phys.* **48** 693
  40. Chen J, Liu S and Zhao J 2011 Synthesis, application and flame retardancy mechanism of a novel flame retardant containing silicon and caged bicyclic phosphate for polyamide 6 *Polym. Degrad. Stab.* **96** 1508
  41. Schartel B and Hull T R 2007 Development of fire-retarded materials — Interpretation of cone calorimeter data *Fire Mater.* **31** 327
  42. Nyambo C, Kandare E, Wang D and Wilkie C A 2008 Flame-retarded polystyrene: Investigating chemical interactions between ammonium polyphosphate and MgAl layered double hydroxide *Polym. Degrad. Stab.* **93** 1656
  43. Hull T R and Kandola B K (Eds.) 2009 *Fire Retardancy of Polymers: New Strategies and Mechanisms* (The Royal Society of Chemistry: UK)
  44. Chigwada G, Kandare E, Wang D, Majoni S, Mlambo D, Wilkie C A and Hossenlopp J M 2008 Thermal stability and degradation kinetics of polystyrene/organically—modified montmorillonite nanocomposites *J. Nanosci. Nanotechnol.* **8** 1927
  45. Chen L and Wang Y-Z 2010 Aryl polyphosphonates: Useful halogen-free flame retardants for polymers *Materials (Basel)* **10** 4746
  46. Kashiwagi T, Du F, Douglas J F, Winey K I, Harris R H and Shields J R 2005 Nanoparticle networks reduce the flammability of polymer nanocomposites *Nat. Mater.* **4** 928
  47. Majoni S, Su S and Hossenlopp J M 2010 The effect of boron-containing layered hydroxy salt (LHS) on the thermal stability and degradation kinetics of poly (methyl methacrylate) *Polym. Degrad. Stab.* **95** 1593